

## Article

# Utilizing Fractional Artificial Neural Networks for Modeling Cancer Cell Behavior

Reza Behinfaraz <sup>1</sup>, Amir Aminzadeh Ghavifekr <sup>2</sup> , Roberto De Fazio <sup>3</sup>  and Paolo Visconti <sup>3,\*</sup> 

<sup>1</sup> Faculty of Electrical and Computer Engineering, Urmia University, Urmia 57561-51818, Iran; r.behinfaraz@urmia.ac.ir

<sup>2</sup> Faculty of Electrical and Computer Engineering, University of Tabriz, Tabriz 51666-16471, Iran; aa.ghavifekr@tabrizu.ac.ir

<sup>3</sup> Department of Innovation Engineering, University of Salento, 73100 Lecce, Italy; roberto.defazio@unisalento.it

\* Correspondence: paolo.visconti@unisalento.it

**Abstract:** In this paper, a novel approach involving a fractional recurrent neural network (RNN) is proposed to achieve the observer-based synchronization of a cancer cell model. According to the properties of recurrent neural networks, our proposed framework serves as a predictive method for the behavior of fractional-order chaotic cancer systems with uncertain orders. Through a stability analysis of weight updating laws, we design a fractional-order Nonlinear Autoregressive with Exogenous Inputs (NARX) network, in which its learning algorithm demonstrates admissible and faster convergence. The main contribution of this paper lies in the development of a fractional neural observer for the fractional-order cancer systems, which is robust in the presence of uncertain orders. The proposed fractional-order model for cancer can capture complex and nonlinear behaviors more accurately than traditional integer-order models. This improved accuracy can provide a more realistic representation of cancer dynamics. Simulation results are presented to demonstrate the effectiveness of the proposed method, where mean square errors of synchronization by applying integer and fractional weight matrix laws are calculated. The density of tumor cell, density of healthy host cell and density of effector immune cell errors for the observer-based synchronization of fractional-order (OSFO) cancer system are less than 0.0.0048, 0.0062 and 0.0068, respectively. Comparative tables are provided to validate the improved accuracy achieved by the proposed framework.

**Keywords:** fractional cancer model; neural network; observer-based synchronization; weight updating laws



**Citation:** Behinfaraz, R.; Ghavifekr, A.A.; De Fazio, R.; Visconti, P.

Utilizing Fractional Artificial Neural Networks for Modeling Cancer Cell Behavior. *Electronics* **2023**, *12*, 4245.

<https://doi.org/10.3390/electronics12204245>

electronics12204245

Academic Editors: Andres Hernandez-Matamoros, Tun-Wen Pai and Hamido Fujita

Received: 18 September 2023

Revised: 9 October 2023

Accepted: 11 October 2023

Published: 13 October 2023



**Copyright:** © 2023 by the authors. Licensee MDPI, Basel, Switzerland. This article is an open access article distributed under the terms and conditions of the Creative Commons Attribution (CC BY) license (<https://creativecommons.org/licenses/by/4.0/>).

## 1. Introduction

Regarding the significant mortality rates associated with cancer, the accurate analysis and detection of tumor behaviors holds immense importance in the field of medicine. Primary investigations [1,2] have laid the foundation for understanding the proliferation of cancer cells. Subsequent to these initial studies, numerous methodologies have been proposed to illustrate the diverse behaviors exhibited by cancer cells under varying conditions [3,4]. Many studies have utilized mathematical frameworks to comprehensively model the dynamics of cancer cells, which have proven to be a valuable tool in formulating precise properties that capture the complexities inherent in cancer cell growth [5]. Cancer represents a complex phenomenon in which numerous factors interact across extensive spatial and temporal dimensions. Clinical data cannot always uncover the underlying mechanisms behind the observed occurrences. In [6], the importance of mathematical modeling as a powerful tool in interpreting these data is highlighted, and several case studies are presented for theoretical models of solid tumor growth. Extending this study, multi-scale models of solid tumor growth are provided in [7].

The chaotic nature of time series [8] has been applied to demonstrate that cancer cells exhibit chaotic behavioral patterns [9]. In addition, observer-based synchronization [10]

stands as a conventional technique employed to elucidate the complex dynamics and is one of the most common methods of specifying the behavior of cancer cell growth. An emerging paradigm in this field involves the fractional modeling of chaotic systems, introducing a novel approach with distinct properties [11].

The properties of fractional calculations make the fractional-order modeling more accurate in numerous natural and practical systems. As a result, fractional-order modeling has found applications in various biological systems [12,13]. Examples of these applications include fractional-order biological population models [14], fractional models for epidemics [15] and fractional models used in control strategies during an outbreak of dengue fever [16]. There has been a significant increase in the exploration of fractional-order chaotic systems and their diverse applications [17].

Adaptive global synchronization within a predetermined time interval for two chaotic systems with fractional-order dynamics and time delays is proposed in [18]. In [19], a comprehensive examination of a novel fractional-order chaotic system driven by a chaos entanglement function is conducted through multiple analytical tools. Moreover, a novel finite-time terminal observer is designed in this study for the estimation of the state variables of the fractional-order system. Evolutionary algorithms have been utilized in [20] for the parameter and order estimation of fractional-order chaotic systems. A novel adaptation law is introduced in [21] to overcome the synchronization problem in a class of nonlinear fractional-order systems with chaotic behavior within the context of fractional-order sliding mode control. The key novelty in this study is the selection of a sliding surface characterized by two adaptable parameters.

One notable biological model of fractional-order chaotic systems is the cancer system model. Recent investigations have focused on the fractional version of the cancer model, achieving a commendable level of accuracy when compared to real-world data concerning cancer cells [22,23]. One of the most important applications of chaotic systems is chaos synchronization. We have previously developed mathematical models to achieve synchronization in fractional-order systems [24,25]. The observer-based synchronization of fractional-order (OSFO) chaotic systems has also been performed using various approaches [26]. All of these methods involve analytical techniques with complex calculations. While the results demonstrate successful synchronization, there are instances where refinement through modifications could lead to improved outcomes.

Artificial neural networks present a promising outcome for the modeling of complex systems or those with unknown specifications [27]. Recent emerging techniques such as the 3D mesh learning method [28] and perceptual metric-guided generative adversarial networks [29] have improved their efficacy further. The development of a neural network identifier is outlined in [30], which operates in the complex domain for uncertain nonlinear systems. This algorithm is derived from a specific class of controlled Lyapunov functions. Different types of artificial neural networks have been introduced for various applications. Neural networks used in predicting nonlinear systems operate in a nonparametric manner, eliminating the need for precise knowledge about the system specifications. Previous studies have explored the integration of artificial neural networks into observer design for nonlinear systems [31]. In [32], an adaptive neural network-based decentralized output feedback control system for interconnected nonlinear systems with strict feedback dynamics and uncertain parameters is designed. This system involves variable virtual and control gain functions, and neural networks are employed to approximate unknown nonlinearities. Moreover, an adaptive neural control with fixed-time convergence for a specific class of uncertain nonlinear systems is proposed in [33], which takes into account the hysteresis input and unobservable states. While artificial neural networks are widely used in cancer research for tasks like cancer classification, their application to model the behavior of cancer cells represents a novel and emerging focus [34,35]. One of the most common types of artificial neural networks used in time series predictions is the adaptive recurrent neural network (RNN) [36]. These networks, with a sufficient number of neurons, can be used for the realization of nonlinear systems [37]. Fractional-order forms of RNNs have been extended

for the modeling of complex systems. They have the potential to make significant contributions to various biological fields due to their ability to model complex and non-integer order dynamics. These networks offer several benefits compared to simple artificial neural networks or recurrent neural networks when it comes to cancer modeling. They are better equipped to model the complex and non-integer-order dynamics present in cancer systems. They can model long-range dependencies, memory effects and fractional-order differential equations more accurately. Fractional-order neural networks can improve parameter estimation in cancer models. They can help to identify fractional-order parameters that may be overlooked by traditional integer-order models, leading to more accurate parameter values and more reliable model predictions. For instance, fractional neural networks can be used to analyze and process biological signals such as electroencephalograms (EEGs) [38]. Moreover, they can be utilized to model the interactions between drugs and biological systems. They can help in predicting the efficacy and side effects of drugs, optimizing drug dosages and identifying potential drug candidates [39]. These networks can improve image processing and analysis in medical imaging applications. They can enhance feature extraction and disease detection in modalities such as MRI, CT and ultrasound [40].

The primary purpose of predicting nonlinear systems is to create a model that can approximate the system. The chaotic behavior and fractional aspects of a system amplify its complexity. This complexity makes predicting system behavior a more challenging task for artificial neural networks. The Nonlinear Autoregressive with Exogenous Inputs (NARX) network is a type of neural network with unique properties [41]. These properties make this type of neural network a good choice to predict the behavior of fractional-order chaotic systems. Cancer is a complex and multifaceted disease that exhibits non-integer-order dynamics in several aspects of its progression. Traditional mathematical models based on integer-order differential equations cannot analyze the intricate behaviors of cancer systems accurately. Our research addresses this gap by introducing the use of fractional neural networks, which are capable of modeling and capturing the fractional-order dynamics in cancer. Utilizing the proposed method, we aim to improve our understanding of cancer's complexity and develop more accurate models. The application of fractional-order neural networks is relatively novel in modeling biological systems. The flexibility of fractional-order calculations in the design of weight update laws helps us to achieve greater accuracy and robustness in neural network design. The main focus of this paper is to design a neural network with fractional-order weight updates for the fast and reliable detection of the behaviors of fractional-order cancer cells, even in cases with uncertain orders. Fractional-order models can capture the complex, non-integer-order dynamics that are often present in biological systems. They provide a more accurate representation of the intricate behaviors of cancer cells. In this study, utilizing the stability analysis of fractional-order systems, sufficient stability conditions are provided to achieve weight update laws for a fractional-order cancer system. Through the application of the proposed stability analysis, it is revealed that the connection weights within the NARX network converge towards their optimal values. This outcome demonstrates the effectiveness of the designed observer.

The main contributions of this paper are as follows:

- The proposed method for observer-based synchronization in incommensurate fractional-order systems is based on a fractional recurrent neural network;
- The proposed method is robust in the presence of uncertain orders;
- A novel stability analysis for the stability of fractional-order systems is introduced;
- The proposed stability analysis is applied to fractional-order systems with uncertain orders;
- Based on the case study, a fractional-order updating rule is proposed for the designed artificial neural networks, which enhances the network's performance.

The rest of the paper is organized as follows. In Section 2, basic definitions related to fractional calculus and cancer cells are introduced, followed by the presentation of a fractional model for cancer. Section 3 introduces the observer design based on artificial neural networks and provides the mathematical relations of this network. Section 4 presents

the stability analysis for the designed network, specifically focusing on the updating procedure of the connection weights within the neural network. Moving to Section 5, an illustrative example is provided to validate the method’s effectiveness, and then the discussion of these results is given in Section 6. Finally, in Section 7, the main conclusions of the study are provided.

## 2. Basic Definition

### 2.1. Mathematical Model of Cancer

The model of cancer cells is obtained by the progression and regression of a tumor. The effective parameters in this model are lymphocytes, macrophages and anticancer agent cells. Macrophages circulate around the body with the cardiovascular system, and all tissues of the body may contain macrophages [42,43]. The main idea of cancer modeling is obtained from a prey–predator-like system. The predator includes cytotoxic macrophages and T-lymphocytes. The predator attacks the tumor cells and destroys them. After this, macrophages release cytokines and activate T-lymphocytes. The predator contains two hunting and resting cells. The resting cells directly do not have ability to destroy tumor cells and usually are converted into T-lymphocytes.

Mathematically, the conversion of cells is depicted through a direct action. Additionally, employing the law of mass action, the obliteration of tumor cells can be quantified as the rate of their depletion. This comprehensive model captures the intricate dynamics of tumor interactions and transformations.

According to the mentioned description, a mathematical model as below can show the desired behavior.

$$\begin{cases} \dot{T} = c_1T(1 - c_2^{-1}T) - c_3NT - c_4TI \\ \dot{N} = c_5N(1 - c_6^{-1}N) - c_7TN \\ \dot{I} = M + \frac{c_8IT}{c_9+T} - c_9IT - c_{10}I \end{cases} \quad (1)$$

where  $T(t)$  is the density of tumor cells,  $N(t)$  is the density of healthy host cells and  $I(t)$  is the density of effector immune cells.

The first equation of system (1) shows the changes in tumor cells with time. The first term of this equation shows the growth of tumor cells without any effect.  $c_1$  is the rate of growth and  $c_2$  is the maximum carrying capacity. The next term,  $c_3NT$ , is the coefficient of competition between host and tumor cells. Moreover, the competition between immune cells and tumor cells is shown in term  $c_4TI$ .

Like the first equation, the first term of the second equation shows the growth of healthy cells with rate  $c_5$  and maximum carrying capacity  $c_6$ . In general,  $c_1 > c_6$ , which means that cancer cells grow faster than healthy cells. Here, again, the competition between healthy and tumor cells is shown with coefficient  $c_7$  in the second term. In the second equation,  $M$  shows the stimulation of immune cells. This stimulation occurs with tumor-specified antigens.  $c_8$  and  $c_9$  are positive constants that show the recognition process of tumor cells by the immune system. The interaction of immune cells and tumor cells is shown in the third term of the third equation, with the  $c_9$  coefficient. Moreover,  $c_{10}$  shows the natural rate of destruction of immune cells.

For  $M = 0$ , we can write the cancer model in Equation (1) as [43]

$$\begin{cases} \dot{x}_1 = x_1(1 - x_1) - k_1x_1x_2 - k_2x_1x_3 \\ \dot{x}_2 = k_3x_2(1 - x_2) - k_4x_1x_2 \\ \dot{x}_3 = \frac{k_5x_1x_3}{k_6+x_3} - k_7x_1x_3 - k_8x_3 \end{cases} \quad (2)$$

where  $k_1 = c_3/c_1$ ,  $k_2 = c_4/c_1$ ,  $k_3 = c_5/c_6$ ,  $k_4 = c_7/c_5$ ,  $k_5 = c_8$ ,  $k_6 = c_9$ ,  $k_7 = c_9$  and  $k_8 = c_{10}$ .

### 2.2. Fractional-Order Systems

Fractional calculus is the general form of ordinary calculations. In this type of calculation, the orders of differential equations are fractional. To describe this type of differential equation, we must define fractional operators. There are several definitions of a fractional operator. One prevalent definition characterizes fractional operators as [44]

$$D_t^q F(t) = \lim_{h \rightarrow 0} h^{-q} \sum_{k=0}^{(t-[q]-1)/h} (-1)^k \binom{q}{k} F(t - kh) \tag{3}$$

where  $\binom{q}{k} = \frac{q(q-1)\dots(q-k+1)}{k!}$ . This definition of a fractional operator is known as the Grunwald–Letnikov definition [44].

### 2.3. Numerical Method for Fractional-Order Systems

According to the absence of analytical solutions for fractional-order differential equations, it becomes necessary to employ approximation techniques in order to solve this category of differential equation. Several methods have been devised to tackle such equations. In the context of this paper, the Adams–Bashforth–Moulton method is adopted as the means to solve fractional-order differential equations [25]. To clarify this approach, we consider the following differential equation:

$$D^q x(t) = f(t, x(t)), \quad 0 \leq t \leq T \tag{4}$$

and

$$x^{(k')}(0) = x_0^{(k')}, \quad k' = 0, 1, \dots, n - 1 \tag{5}$$

Here,  $q$  shows the fractional order,  $f$  represents the function and  $m$  is the first integer number larger than  $q$ . This differential equation is equivalent to the Volterra integral equation as [34]

$$x(t) = \sum_{k'=0}^{m-1} x_0^{(k')} \frac{t^{k'}}{k'!} + \frac{1}{\Gamma(q)} \int_0^t (t-s)^{q-1} f(s, y(s)) ds \tag{6}$$

We consider  $h = T/N$ ,  $t_k = kh$  ( $k = 0, 1, 2, \dots, N$ ), and Equation (6) can be discretized as follows:

$$x_h(t_{k+1}) = \sum_{k'=0}^{m-1} x_0^{(k')} \frac{t_{k+1}^{k'}}{k'!} + \frac{h^q}{\Gamma(q+2)} f(t_{n+1}, x_h^P(t_{n+1})) + \frac{h^q}{\Gamma(q+2)} \sum_{j=0}^n a_{j,n+1} f(t_j, x_h^P(t_j)) \tag{7}$$

where the predicted value  $x_h(t_{n+1})$  is determined by

$$x_h^P(t_{n+1}) = \sum_{k=0}^{m-1} x_0^{(k')} \frac{t_{k+1}^k}{k!} + \frac{1}{\Gamma(q)} \sum_{j=0}^k b_{j,k+1} f(t_j, y_h(t_j)) \tag{8}$$

in which

$$a_{j,k+1} = \begin{cases} k^{q+1} - (k-q)(k+1)^q, & j = 0 \\ (k-j+2)^{q+1} + (k-j)^{q+1} - 2(k-j+1)^{q+1}, & 1 \leq j \leq N \\ 1, & j = k+1 \end{cases} \tag{9}$$

$$b_{j,k+1} = \frac{h^q}{q} ((k+1-j)^q (k-j)^q) \tag{10}$$

The description of the approximation error in this estimation is as follows:

$$\max|x(t_j) - x_h(t_j)| = o(h^b)$$

where  $b = \min(2, 1 + q)$ .

### 2.4. Fractional Version of Cancer System

As mentioned in the previous section, the fractional modeling of many systems is more accurate than the integer version. The fractional version of system (2) can be written as [45]

$$\begin{cases} \frac{d^{q_1+\delta q_1}}{dt} x_1 = x_1(1 - x_1) - k_1x_1x_2 - k_2x_1x_3 \\ \frac{d^{q_2+\delta q_2}}{dt} x_2 = k_3x_2(1 - x_2) - k_4x_1x_2 \\ \frac{d^{q_3+\delta q_3}}{dt} x_3 = \frac{k_5x_1x_3}{k_6+x_3} - k_7x_1x_3 - k_8x_3 \end{cases} \quad (11)$$

The parameters and states of system (2) are similar to those of system (11).  $\delta q_1, \delta q_2, \delta q_3$  are the uncertainty of orders. For certain incommensurate orders such as  $(q_1, q_2, q_3) = (0.97, 0.95, 0.97)$ , the chaotic behavior of the system is as shown in Figure 1.

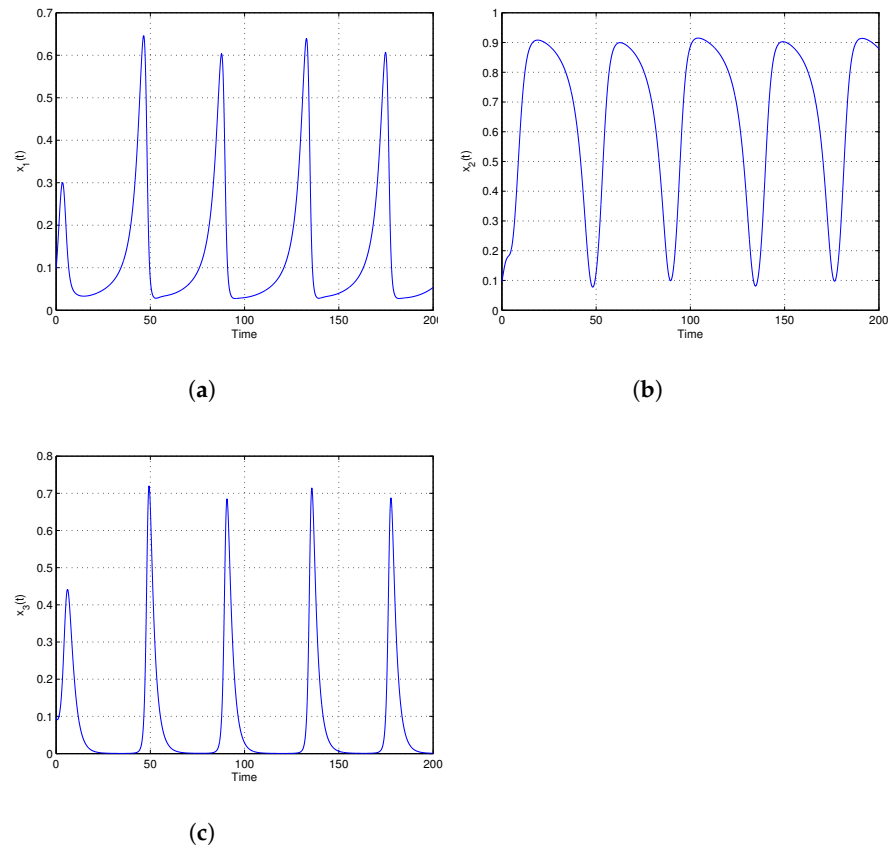


Figure 1. Chaotic behavior of fractional-order cancer system (a)  $x_1$ , (b)  $x_2$ , (c)  $x_3$ .

### 3. Observer Design with Neural Networks

In the previous section, the fundamental concepts of a fractional-order cancer cell model are defined. In this section, the relations and structure of the fractional-based neural network will be presented and the stability analysis will be described.

Neural networks have the ability to approximate a nonlinear function with a bounded error dynamic. A nonlinear function can be written as follows:

$$g(Y) = X\alpha(Y) + \beta(Y) \quad (12)$$

In this expression,  $g(Y)$  signifies a nonlinear function,  $X$  denotes the constant ideal weight matrix and  $\alpha(\cdot)$  represents the basis function. Additionally,  $\beta$  stands for the bounded error. The estimation of the nonlinear function (12) through the utilization of artificial neural networks is articulated as

$$\hat{g}(\hat{Y}) = \hat{X}\alpha(\hat{Y}) \tag{13}$$

where  $\hat{X}$  is obtained through the training of the neural network. The estimation error can be represented as

$$E = X\alpha(Y) + \beta(Y) - \hat{X}\alpha(\hat{Y}) \tag{14}$$

In the following, we use this estimation error in a synchronization problem.

### 3.1. Observer-Based Synchronization

Here, we propose the observer-based synchronization in fractional-order chaotic systems. A fractional-order chaotic system in general form can be shown as

$$D^q Y = AY + g(Y) \tag{15}$$

where  $Y$  shows the states of the system,  $A$  is the linear part and  $g$  is the nonlinear part, which is estimated by the neural network.

For the estimated system, we have the following system:

$$D^q \hat{Y} = A\hat{Y} + \hat{g}(\hat{Y}) + u \tag{16}$$

where  $\hat{Y}$  represents the vector of estimated states,  $\hat{g}$  signifies the estimation of the nonlinear component and  $u$  denotes an additional control signal incorporated into the estimated system to ensure the convergence of the estimation process. Then, the synchronization error of the designed observer is

$$D^q E = AE + \hat{g}(\hat{Y}) - g(Y) + u \tag{17}$$

Taking into consideration the estimation error associated with the nonlinear component as expressed in Equation (14), we can rephrase Equation (17) in the following manner:

$$D^q E = AE + X\alpha(Y) + \beta(Y) - \hat{X}\alpha(\hat{Y}) + u \tag{18}$$

By introducing the terms  $X\alpha(\hat{Y})$  and performing both addition and subtraction to Equation (18), we obtain

$$D^q E = AE + \bar{X}\alpha(\hat{Y}) + X_1(t) + \beta(Y) + u \tag{19}$$

where  $\bar{X} = X - \hat{X}$  and

$$X_1(t) = X(\alpha(Y) - \alpha(\hat{Y}))$$

In the general context, and particularly in cases of chaos,  $X_1(t)$  is known to be bounded. By choosing an appropriate control signal  $u$ , in the designed neural network observer, the error of estimated weights converges to zero. The block diagram of the observer-based synchronization based on neural networks is shown in Figure 2. In this figure, the *NN* block represents the designed NARX neural network, which is a recurrent network, and the details of this network will be discussed in the next section. The  $g(y)$  block is used to show the nonlinear vector of the fractional-order cancer model, which is formulated in Equation (11) as follows:

$$g(y) = \begin{bmatrix} -y_1^2 - k_1 y_1 y_2 - k_2 y_1 y_3 \\ -k_3 y_2^2 - k_4 y_1 y_2 \\ \frac{k_5 y_1 y_3}{k_6 + y_3} - k_7 y_1 y_3 \end{bmatrix} \tag{20}$$

The FOI block denotes the fractional-order integrator, which uses the Grunwald–Letnikov definition of the fractional order operator.

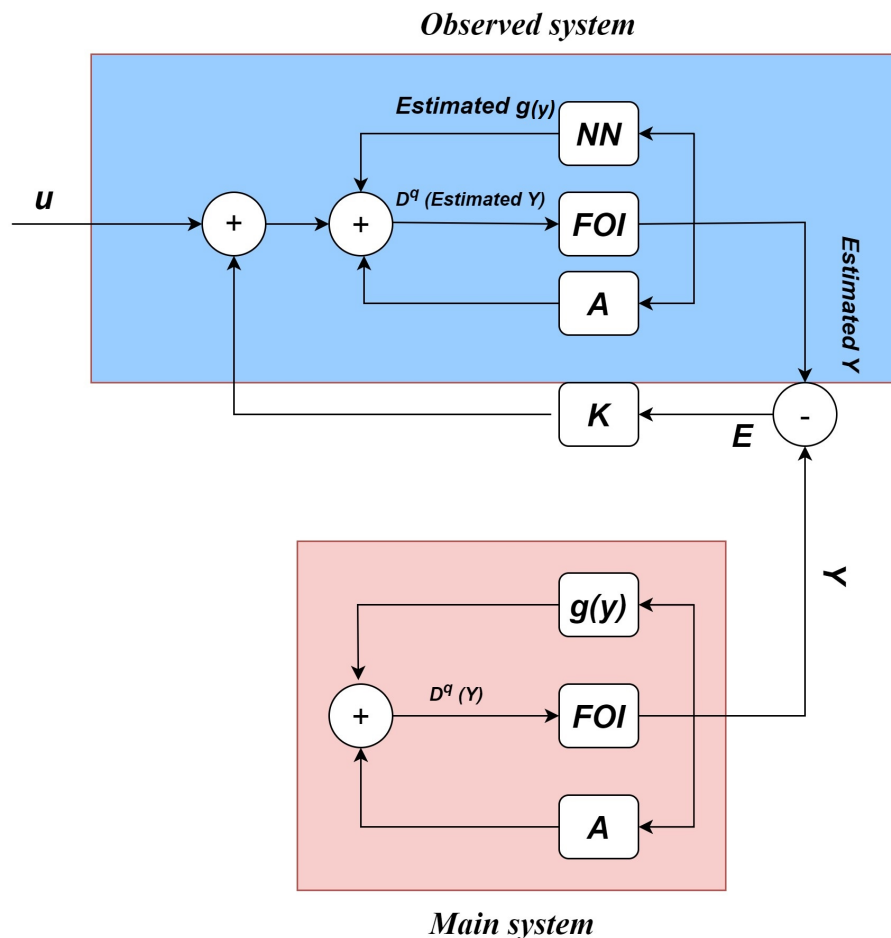


**Figure 2.** Schematic of the observer-based synchronization. NN: Neural Network; FOI: Fractional Order Integrator ( $K$  is the matrix of coefficient of control signals).

### 3.2. Structure of Observer-Based Synchronization with Neural Network

In this arrangement, each state of the nonlinear system at the discrete time instant  $t$  is associated with previous time samples in the following manner:

$$Y(t) = g(Y(t - 1), \dots, Y(t - n_Y)) \tag{21}$$

where  $Y$  signifies the model’s states at a discrete time step  $t$ . Additionally, within this model,  $n_Y \geq 1$  denotes the number of memory delays for the states, while  $g$  represents a nonlinear function. Notably, this function is approximated through a multilayer perceptron (MLP). The NARX network comprises an embedded MLP network, which in turn has connections with independent inputs and past outputs for output computation. As depicted in Figure 3, this network defines system feedback by utilizing both the system output and independent input. Notably, there is no feedback loop involving the outputs of the hidden layer of the network. Nevertheless, the NARX network’s output exhibits greater accuracy compared to other forms of recurrent neural networks [46]. This model is illustrated in Figure 3. Within this architecture,  $X_1$  denotes the input weight matrix in the hidden layer,  $X_2$  represents the network output feedback weight matrix in the hidden layer and  $X_3$  corresponds to the weight matrix in the output layer. Importantly, it becomes evident that by selecting the requisite number of observers for each state, alongside a suitable number of samples ( $n_Y$ ),



the estimation of the nonlinear components within the system (15) can be achieved with an acceptable level of error.

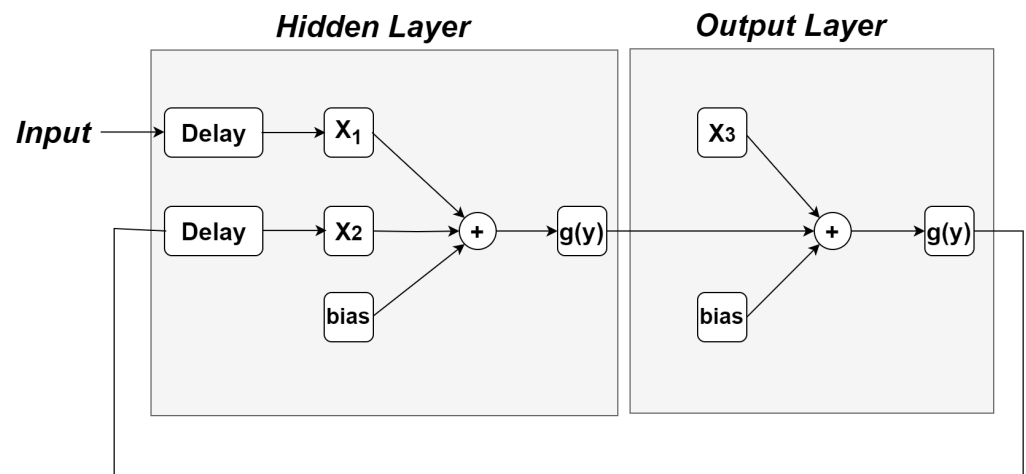


Figure 3. Structure of NARX neural network [46].

#### 4. Stability Analysis and Weight Update Rule

##### 4.1. Fundamental Principles of Stability in Fractional-Order Systems

In the case of a generic fractional differential equation,

$$D^q y(t) = g(y) \tag{22}$$

the Lyapunov stability theory applicable to the system (22) is as follows.

**Theorem 1.** With fractional-order  $q \in (0, 1]$ , for a positive definite  $V(y(t))$ , if there is a semi-negative definite  $D^q V(y(t))$ , then system (22) is Lyapunov stable [47].

The Leibniz rule [48] stands as a well-recognized concept in fractional calculus. It elucidates fractional differentiation for the product of two functions as the following:

$$D^q (f \cdot g) = \sum_{n=0}^{\infty} \binom{q}{n} D^{q-n} f \cdot D^n g \tag{23}$$

where

$$\binom{q}{n} = \frac{\Gamma(q+1)}{\Gamma(q-n+1)\Gamma(n+1)} \tag{24}$$

When aiming to multiply two similar functions, the Leibniz rule can be articulated as follows:

$$D^q (g^2) = \sum_{n=0}^{\infty} \binom{q}{n} D^{q-n} g \cdot D^n g \tag{25}$$

An other form of Equation (25) is

$$D^q (g^2) = \sum_{n=0}^{\infty} \binom{q}{n} D^q g \cdot D^0 g \tag{26}$$

Regarding the subsequent relationships concerning the stability of fractional-order systems, it is pertinent to note that for a complex value of  $q$  and  $|x| < 1$ , the related binomial series is introduced as

$$(1 + y)^q = \sum_{n=0}^{\infty} \binom{q}{n} y^n \tag{27}$$

The convergence of the series for  $y = 1$  is guaranteed when  $Re(q) > -1$ . In this case, we have  $q \in (0, 1)$ , and

$$(1 + 1)^q = \sum_{n=0}^{\infty} \binom{q}{n} \tag{28}$$

Then, Equation (26) can be written as

$$D^q(g^2) = 2^\alpha D^q g \cdot g \tag{29}$$

By considering a Lyapanov candidate function for the estimation error (19) as

$$V = E^2 \tag{30}$$

for this positive defined function, by using Equation (29), we have

$$D^q V = 2^q D^\alpha E E \tag{31}$$

Now, by using Equation (19), and choosing an appropriate  $u$ , we obtain  $D^q V \leq 0$ . This signifies the successful functioning of the designed observer, thereby accomplishing observer-based synchronization. An effective option for  $u$  can be set as  $u = -X_1(t) - \beta(Y) - KE$ . This particular choice of  $u$  yields  $D^q E E = (A - K)E^2$ , which indicates that, through a well-chosen  $K$ , the error converges to zero, ensuring the robust performance of the synchronization process.

#### 4.2. Analysis of Updating Rules

To ensure the effective training of each neural network, it is crucial to develop a proper learning algorithm. The core concept of training neural networks relies on defining an appropriate update rule for the adjustment of connection weights. In this case, this update rule is essential to guarantee the proper functioning of the designed observer. Among the well-established algorithms, the back-propagation algorithm [46] stands out as a noteworthy choice for updating weights. Based on this algorithm, we can propose the following theorem to provide a stable neural observer.

**Theorem 2.** *Considering the model (11) alongside observer (16), and adopting a learning rate denoted by  $\rho$ , the fractional updating rule takes the form*

$$D^q \hat{X} = -\rho(E^T A_p^{-1})^T \sigma(\hat{Y})^T - \epsilon ||E|| \hat{X} \tag{32}$$

Here,  $\epsilon$  represents a small positive constant,  $A_p = A - K$  retains the same definition as mentioned in the previous subsection, and  $q \in (0, 1]$ . Consequently, the convergence of the estimation error (1) to zero can be successfully attained.

**Proof.** Following the stability criteria delineated in fractional differential Equation (31) for a quadratic function, it becomes evident that when the system order lies within the range of  $(0, 1]$ , the stability observed in the integer version extends to the fractional variant. Consequently, fractional-order systems can accommodate uncertain orders provided that these orders remain below 1. The integer representation of Equation (32) is expressed as

$$\dot{\hat{X}} = -\rho(E^T A_p^{-1})^T \alpha(\hat{Y})^T - \gamma ||E|| \hat{X} \tag{33}$$

Expressing the weight error matrix as  $\bar{X} = X - \hat{X}$ , we can derive simplified relationships as follows:

$$\dot{\bar{X}} = -\rho(E^T A_p^{-1})^T \alpha(\hat{Y})^T + \gamma ||E|| \hat{X} \tag{34}$$

For a Lyapunov function as

$$V = E^T P_s E + tr(\bar{X}^T \gamma^{-1} \bar{X}) \tag{35}$$

where  $P_s$  is a positive definite matrix, the derivative of the Lyapunov function can be calculated as

$$\dot{V} = \dot{E}^T P_s E + E^T P_s \dot{E} + tr(\bar{X}^T \epsilon^{-1} \dot{\bar{X}}) \tag{36}$$

The matrix  $P_s$  fulfills the condition (37) in the presence of a positive definite matrix  $Q_s$ .

$$A_p^T P_s + P_s A_p = -Q_s \tag{37}$$

Then, using Equation (19) and Equations (32) and (37), we have

$$\dot{V} = -\dot{E}^T Q_s E + E^T P_s (\bar{C}\alpha(\hat{Y}) + X_1(t) + \beta(Y)) + tr(\bar{X}^T M E \alpha^T + \bar{X} \|E\| (X - \bar{X})) \tag{38}$$

where  $M = \rho \epsilon A_p^{-T}$ . Moreover, we have

$$tr(\bar{X}^T (X - \bar{X})) \leq C_1 \|\bar{X}\| - \|\bar{X}\|^2 \tag{39}$$

$$tr(\bar{X}^T M E \alpha^T) \leq C_2 \|\bar{X}^T\| \|M\| \|E\| \tag{40}$$

Here, the coefficients represent two important factors.  $C_1$  is the upper bound of  $X$ , and  $C_2$  is related to the active functions and shows its upper bound. Now, we rewrite Equation (36) as

$$\dot{V} \leq -\lambda_{min}(Q_s) \|E\|^2 + \|E\| \|P_s\| (C_2 \|\bar{X}\| + X_1(t) + \beta(Y)) + C_2 \|\bar{X}\| \|M\| \|E\| + (C_1 \|\bar{X}\| - \|X\|^2) \|E\| \tag{41}$$

where

$$\|E\| \geq (2\|P_s\| (X_1(t) + \beta(Y)) + ((C_2(\|P_s\| + \|M\|)) + C_1)^2 / 2) / \lambda_{min}(Q_s) \tag{42}$$

This can be demonstrated in a more comprehensive manner. Under this circumstance,  $\dot{V}$  takes on a negative definite form, underscoring the convergence of  $E$ . Returning to the equation, we can once again rephrase Equation (34) as

$$\dot{\bar{X}} = f(E) + \epsilon \|E\| \hat{X} = g(E) + \sigma X - \sigma \bar{X} \tag{43}$$

Here,  $X$  remains fixed and  $f = -\rho(E^T A_p^{-1})^T \alpha(\hat{Y})^T$  is bounded. Given the positive  $\sigma$ , we can infer that the system exhibits stability, thus affirming the convergence of the estimated weights to their respective values.

The stability of observer errors can be demonstrated for the integer-order updating rule (33). Building on the insights from the previous subsection regarding fractional order in the range  $(0, 1]$ , this establishes that the weight updating rule with fractional order (32) can be effectively employed as the update rule for NARX neural networks. This comprehensive proof substantiates the viability and effectiveness of the proposed approach.  $\square$

### 5. Simulation and Implementation

According to the general form of fractional-order system (15), the different parts of cancer system (11) can be written as

$$Y = [y_1, y_2, y_3]^T, \quad q = [q_1, q_2, q_3]^T, \quad A = \begin{pmatrix} 1 & 0 & 0 \\ 0 & k_3 & 0 \\ 0 & 0 & -k_7 \end{pmatrix}, \quad f = \begin{pmatrix} -y_1^2 - k_1 y_1 y_2 - k_2 y_1 y_3 \\ k_3 y_2^2 - k_4 y_1 y_2 \\ \frac{k_4 y_1 y_3}{k_5 + y_3} - k_6 y_1 y_3 \end{pmatrix}$$

In this section, we consider fractional-order cancer system (15) with orders and parameters as mentioned in Table 1.

**Table 1.** Order and parameter values.

$q_1$	$q_2$	$q_3$	$k_1$	$k_2$	$k_3$	$k_4$	$k_5$	$k_6$	$k_7$	$k_8$
0.97	0.95	0.97	1	2.5	0.6	1.5	4.5	1	0.2	0.5

Order uncertainty is considered as  $\delta q_i = 0.005\sin(10t)$  and  $\delta q_i = 0.008\sin(10t)$  for  $i = 1, 2, 3$  in the two cases. Moreover, as mentioned in Section 4.1, the matrix  $K$  in the additional control signal is considered as  $K = \text{diag}(-10, -10, -10)$ . With this  $K$ , the convergence of the observer to real states is guaranteed. For the nonlinear part's estimation of this system, we use a neural network with two hidden layers, with each one having 5 neurons. Additionally, a time step of 0.0005 s is taken into account during the discretization process. The number of delayed feedbacks that are affected in each state output is selected as 200 samples. As shown in Figure 4, the convergence of estimation occurs in an acceptable time. We also simulated the problem for the case without uncertainty in the fractional orders. We calculated the mean square error of the proposed method for two systems. The results of these systems are shown in Table 2.

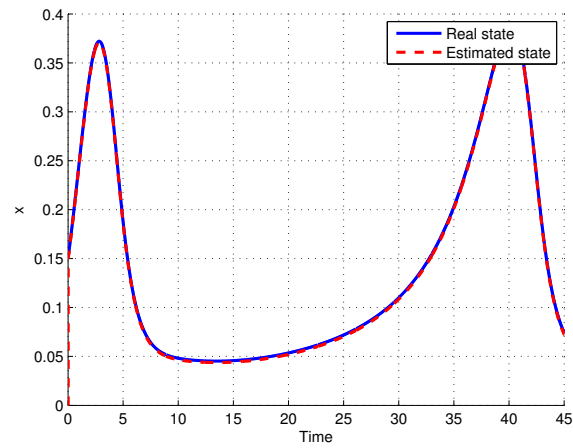
**Table 2.** Comparison of mean square error for OSFO cancer systems with different order uncertainty.

	$e_1$	$e_2$	$e_3$
OSFO without order uncertainty	0.0016	0.0024	0.0035
OSFO with order uncertainty ( $\delta q_i = 0.005\sin(10t)$ )	0.0048	0.0062	0.0068
OSFO with order uncertainty ( $\delta q_i = 0.008\sin(10t)$ )	0.0125	0.0162	0.0174

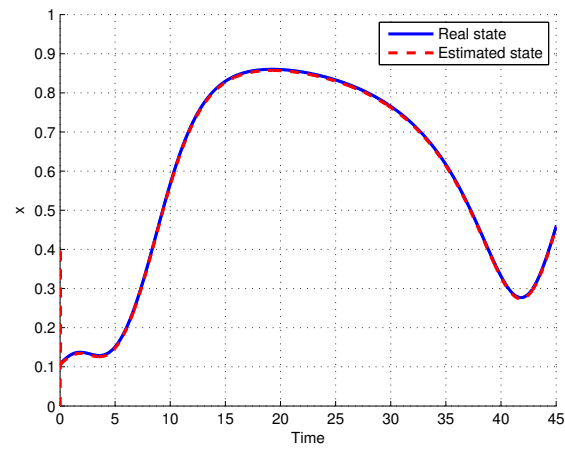
We simulate this example with a fractional-order RNN and ANN. In addition, we simulate it with an integer-order RNN. The results of these simulations are shown in Table 3. The observer-based synchronization errors when applying an integer weight matrix update law as in Equation (33) and a fractional weight matrix update law as in Equation (32) are illustrated in Figure 5. As shown in this figure, the fractional update law leads to better results. To make a comparison, we simulate this problem using the approach outlined in [43]. This paper uses a type 2 active control method to design the observer for synchronization. This network has a feedforward structure without any complexity. The errors of synchronization when applying this method to the considered case study are shown in Figure 6, which shows that it cannot achieve the observer-based synchronization of fractional-order systems.

**Table 3.** Comparison of mean square error for OSFO cancer systems.

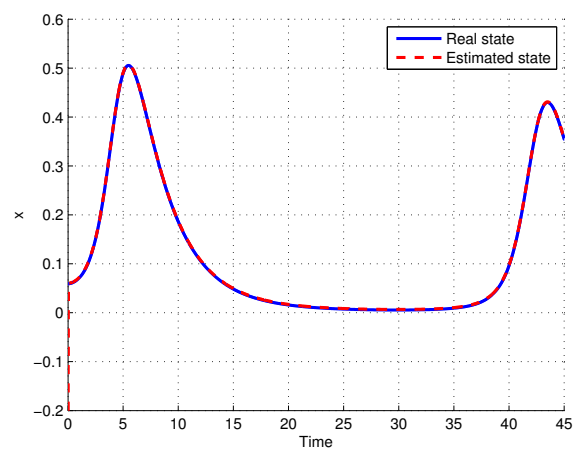
Method	$e_1$	$e_2$	$e_3$
OSFO with integer-order RNN	0.0064	0.0073	0.0088
OSFO with fractional-order ANN	0.0066	0.0084	0.0105
OSFO with fractional-order RNN	0.0048	0.0062	0.0068
OSFO cancer system with Ref. [43] method	1.2251	4.0245	2.3245



(a)

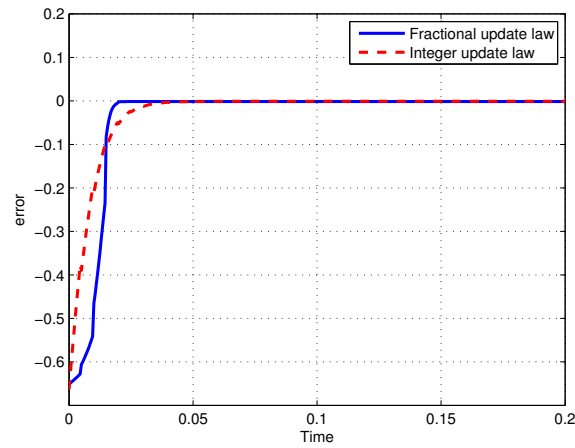


(b)

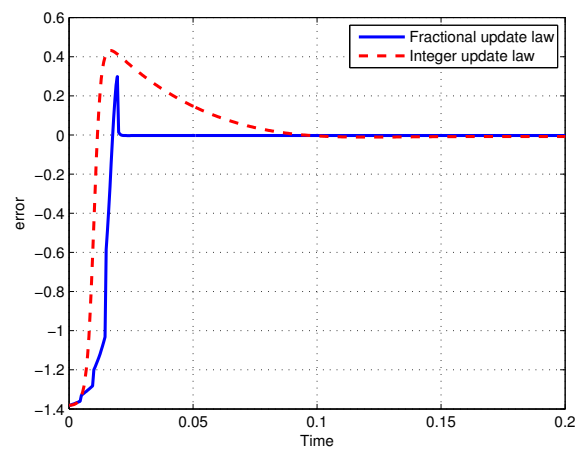


(c)

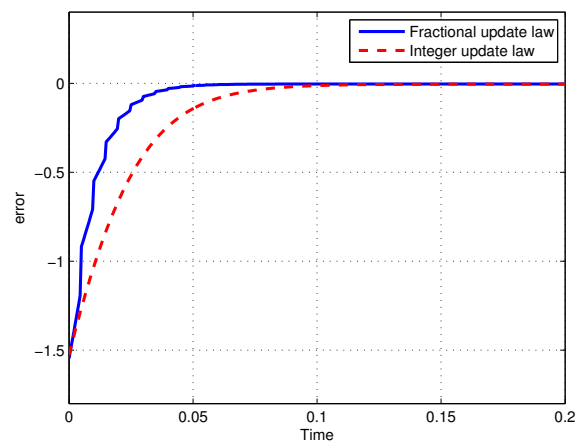
Figure 4. OSFO cancer system (a)  $x_1$ , (b)  $x_2$ , (c)  $x_3$ .



(a)

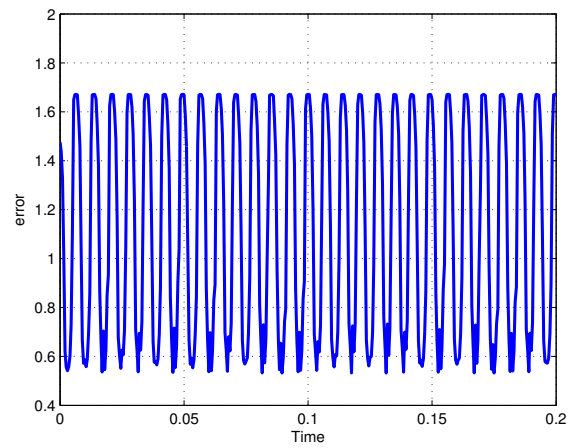


(b)

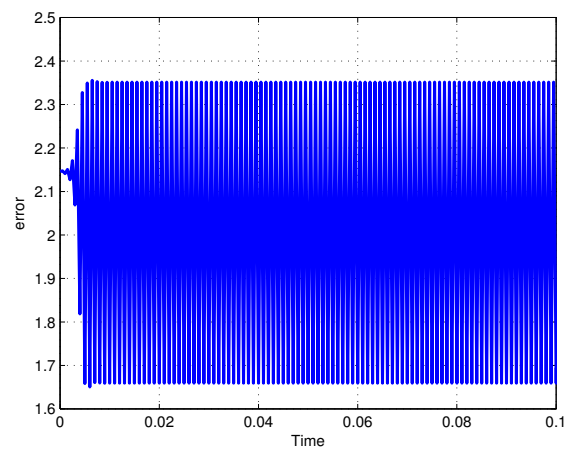


(c)

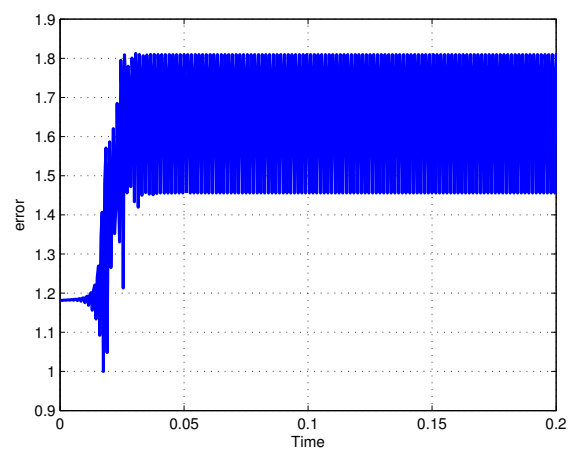
Figure 5. Error of OSFO cancer system (a)  $e_1$ , (b)  $e_2$ , (c)  $e_3$ .



(a)



(b)



(c)

**Figure 6.** Observer-based synchronization error using Ref. [43] method (a)  $e_1$ , (b)  $e_2$ , (c)  $e_3$ .

## 6. Discussion

In the presence of uncertainty in system dynamics, detecting the behavior of the system is a challenging task, especially when this uncertainty is in the order of fractional-order dynamics. In this paper, we have designed an observer using recurrent neural networks to detect the behavior of a fractional-order mathematical cancer model with uncertain fractional orders.

Through stability analysis and the application of fractional rules for weight updates in the neural network, we have achieved a reliable network that exhibits behavior similar to the fractional-order model of cancer cells. The results demonstrate that a neural network can be a promising choice to achieve observer-based synchronization. In the case of a neural network with integer update laws, we achieve an average synchronization time of about 0.05 s. However, this time is reduced to less than 0.03 s when fractional update laws are employed, highlighting the advantages of using fractional-order update laws for neural network weights. Moreover, it is shown that a fractional RNN leads to a better result than a fractional ANN. Fractional artificial networks in cancer modeling offer several potential advantages compared to traditional cancer models, which can be stated as follows.

- \* Fractional-order models can capture complex and nonlinear behaviors more accurately than traditional integer-order models. This improved accuracy can provide a more realistic representation of cancer dynamics.
- \* Fractional-order models offer greater flexibility in representing a wide range of cancer-related phenomena, including tumor growth, metastasis and immune responses. They can adapt to changing conditions and parameters.
- \* Fractional derivatives capture long memory effects, which are essential in modeling phenomena where past events significantly influence the present state, such as tumor evolution and treatment responses.
- \* They can better simulate the multifaceted nature of cancer, accounting for factors like tumor heterogeneity, microenvironment interactions and varying cell behaviors.

Besides all the aforementioned benefits of fractional neural networks, there are some drawbacks and considerations that must be made when using them. A fractional neural network introduces additional complexity to the traditional neural network architecture. The inclusion of fractional-order derivatives and operators can make them more challenging to design and train. Moreover, unlike traditional neural networks, which have well-established architectures and training algorithms, fractional neural networks lack standardization. This can lead to difficulties in replicating results and sharing models among researchers.

To emphasize the performance and novelty of the method of this paper, we simulated another existing method for observer-based synchronization for an uncertain fractional-order cancer model. The compared method was based on type 2 fuzzy active control and the results showed that this method lost its performance in the presence of uncertainties. Moreover, the statistical results for the average synchronization error of the two methods are shown in Table 2. For comparison, we include further simulation results obtained using an integer-order RNN, fractional-order ANN and fractional-order RNN. As seen in Table 3, OSFO with a fractional-order RNN has the best performance in comparison with its similar counterparts.

Like traditional neural networks, fractional artificial networks can inherit biases from the data that they are trained on. Moreover, when dealing with sensitive data, such as medical records, there are ethical concerns about the privacy of individuals. Fractional artificial networks may need to access and process such data, raising issues related to data security and privacy protection. Fractional artificial networks, particularly complex ones, can be difficult to interpret, making it challenging to explain their decisions. This lack of transparency can be problematic, especially in critical domains like healthcare, where decision making should be explainable and justifiable.



## 7. Conclusions

In this paper, the observer-based synchronization of fractional-order chaotic systems with uncertain orders is discussed. The proposed method is based on a fractional recurrent neural network and is applied for chaotic cancer cells. Fractional and integer update laws are used for weight updates, and it is demonstrated that fractional update laws yield superior results. Additionally, we conducted a thorough comparative analysis by comparing our method with an alternative approach to observer-based synchronization using the type 2 fuzzy active control method. The results of this analysis highlighted the limitations of the previous studies, which could not achieve observer-based synchronization in the considered system. On the contrary, our proposed method demonstrated good performance with these challenging conditions. In summary, our research emphasizes the importance of fractional-order techniques in chaos synchronization, demonstrating the effectiveness of our approach even in uncertain situations in fractional-order cancer models.

**Author Contributions:** Conceptualization, R.B.; Methodology, A.A.G.; Validation, R.D.F. and P.V.; Formal analysis, A.A.G.; Investigation, R.B. and P.V.; Resources, A.A.G.; Data curation, R.B. and R.D.F.; Writing—original draft, R.B., A.A.G., R.D.F. and P.V.; Writing—review & editing, R.D.F. and P.V.; Supervision, R.D.F. and P.V.; Funding acquisition, P.V. All authors have read and agreed to the published version of the manuscript.

**Funding:** This research received no external funding.

**Data Availability Statement:** No new data were created in this study.

**Conflicts of Interest:** The authors declare no conflict of interest.

## References

1. Banerjee, S.; Sarkar, R.R. Delay-induced model for tumor-immune interaction and control of malignant tumor growth. *Biosystems* **2008**, *91*, 268–288. [[CrossRef](#)] [[PubMed](#)]
2. Borges, F.S.; Iarosz, K.C.; Ren, H.P.; Batista, A.M.; Baptista, M.S.; Viana, R.L.; Lopes, S.R.; Grebogi, C. Model for tumour growth with treatment by continuous and pulsed chemotherapy. *Biosystems* **2014**, *116*, 43–48. [[CrossRef](#)] [[PubMed](#)]
3. Pham, H. Mathematical modeling the time-delay interactions between tumor viruses and the immune system with the effects of chemotherapy and autoimmune diseases. *Mathematics* **2022**, *10*, 756. [[CrossRef](#)]
4. Das, A.; Dehingia, K.; Sarmah, H.K.; Hosseini, K.; Sadri, K.; Salahshour, S. Analysis of a delay-induced mathematical model of cancer. *Adv. Contin. Discret. Models* **2022**, *2022*, 1–20. [[CrossRef](#)]
5. Metzcar, J.; Wang, Y.; Heiland, R.; Macklin, P. A review of cell-based computational modeling in cancer biology. *JCO Clin. Cancer Inf.* **2019**, *2*, 1–13. [[CrossRef](#)] [[PubMed](#)]
6. Byrne, H.; Alarcon, T.; Owen, M.; Webb, S.; Maini, P. Modelling aspects of cancer dynamics: A review. *Philos. Trans. R. Soc. A Math. Phys. Eng. Sci.* **2006**, *364*, 1563–1578. [[CrossRef](#)]
7. Osborne, J.M.; Walter, A.; Kershaw, S.K.; Mirams, G.R.; Fletcher, A.G.; Pathmanathan, P.; Gavaghan, D.; Jensen, O.E.; Maini, P.K.; Byrne, H.M. A hybrid approach to multi-scale modelling of cancer. *Philos. Trans. R. Soc. A Math. Phys. Eng. Sci.* **2010**, *368*, 5013–5028. [[CrossRef](#)]
8. Ramadevi, B.; Bingi, K. Chaotic time series forecasting approaches using machine learning techniques: A review. *Symmetry* **2022**, *14*, 955. [[CrossRef](#)]
9. Debbouche, N.; Ouannas, A.; Grassi, G.; Al-Hussein, A.B.A.; Tahir, F.R.; Saad, K.M.; Jahanshahi, H.; Aly, A.A. Chaos in cancer tumor growth model with commensurate and incommensurate fractional-order derivatives. *Comput. Math. Methods Med.* **2022**, *2022*, 5227503. [[CrossRef](#)]
10. Liang, J.; Liu, J.; Chen, G. Observer-based synchronization of time-delay complex-variable chaotic systems with complex parameters. *Fractals* **2022**, *30*, 2250197. [[CrossRef](#)]
11. Mohammadi, S.; Hejazi, S.R. Using particle swarm optimization and genetic algorithms for optimal control of non-linear fractional-order chaotic system of cancer cells. *Math. Comput. Simul.* **2023**, *206*, 538–560. [[CrossRef](#)]
12. Al-Nassir, S. Dynamic analysis of a harvested fractional-order biological system with its discretization. *Chaos Solitons Fractals* **2021**, *152*, 111308. [[CrossRef](#)]
13. Debbouche, N.; Ouannas, A.; Momani, S.; Cafagna, D.; Pham, V.-T. Fractional-order biological system: Chaos, multistability and coexisting attractors. *Eur. Phys. J. Spec. Top.* **2021**, *231*, 1061–1070. [[CrossRef](#)]
14. Srivastava, H.; Dubey, V.; Kumar, R.; Singh, J.; Kumar, D.; Baleanu, D. An efficient computational approach for a fractional-order biological population model with carrying capacity. *Chaos Solitons Fractals* **2020**, *138*, 109880. [[CrossRef](#)]
15. Chen, Y.; Liu, F.; Yu, Q.; Li, T. Review of fractional epidemic models. *Appl. Math. Model.* **2021**, *97*, 281–307. [[CrossRef](#)]

16. Jajarmi, A.; Arshad, S.; Baleanu, D. A new fractional modelling and control strategy for the outbreak of dengue fever. *Phys. A Stat. Mech. Its Appl.* **2019**, *535*, 122524. [[CrossRef](#)]
17. Tavazoei, M.S. Fractional order chaotic systems: History, achievements, applications, and future challenges. *Eur. Phys. J. Spec. Top.* **2020**, *229*, 887–904. [[CrossRef](#)]
18. Lin, L.; Wang, Q.; He, B.; Chen, Y.; Peng, X.; Mei, R. Adaptive predefined-time synchronization of two different fractional-order chaotic systems with time-delay. *IEEE Access* **2021**, *9*, 31908–31920. [[CrossRef](#)]
19. Khan, A.; Khan, N. A novel finite-time terminal observer of a fractional-order chaotic system with chaos entanglement function. *Math. Methods Appl. Sci.* **2022**, *45*, 640–656. [[CrossRef](#)]
20. Yousri, D.; AbdelAty, A.M.; Said, L.A.; Elwakil, A.; Maundy, B.; Radwan, A.G. Parameter identification of fractional-order chaotic systems using different meta-heuristic optimization algorithms. *Nonlinear Dyn.* **2019**, *95*, 2491–2542. [[CrossRef](#)]
21. Rabah, K.; Ladaci, S. A fractional adaptive sliding mode control configuration for synchronizing disturbed fractional-order chaotic system. *Circuits Syst. Signal Process.* **2020**, *39*, 1244–1264. [[CrossRef](#)]
22. Alzabut, J.; Selvam, A.G.M.; Dhakshinamoorthy, V.; Mohammadi, H.; Rezapour, S. On chaos of discrete time fractional order host-immune-tumor cells interaction model. *J. Appl. Math. Comput.* **2022**, *68*, 4795–4820. [[CrossRef](#)]
23. Naik, P.A.; Zu, J.; Naik, M.-U.-D. Stability analysis of a fractional-order cancer model with chaotic dynamics. *Int. J. Biomath.* **2021**, *14*, 2150046. [[CrossRef](#)]
24. Behinfaraz, R.; Badamchizadeh, M. Optimal synchronization of two different in-commensurate fractional-order chaotic systems with fractional cost function. *Complexity* **2016**, *21*, 401–416. [[CrossRef](#)]
25. Behinfaraz, R.; Badamchizadeh, M.A. Synchronization of different fractional-ordered chaotic systems using optimized active control. In Proceedings of the 2015 6th International Conference on Modeling, Simulation, and Applied Optimization (ICMSAO), Istanbul, Turkey, 27–29 May 2015; pp. 1–6.
26. Sakthivel, R.; Kwon, O.; Selvaraj, P. Observer-based synchronization of fractional-order Markovian jump multi-weighted complex dynamical networks subject to actuator faults. *J. Frankl. Inst.* **2021**, *358*, 4602–4625. [[CrossRef](#)]
27. Vasilyev, A.; Tarkhov, D. Mathematical models of complex systems on the basis of artificial neural networks. *Nonlinear Phenom. Complex Syst.* **2014**, *17*, 327–335.
28. Li, P.; He, F.; Fan, B.; Song, Y. TPNet: A Novel Mesh Analysis Method via Topology Preservation and Perception Enhancement. *Comput. Aided Geom. Des.* **2023**, *104*, 102219. [[CrossRef](#)]
29. Wu, H.; He, F.; Duan, Y.; Yan, X. Perceptual metric-guided human image generation. *Integr. Comput.-Aided Eng.* **2022**, *29*, 141–151. [[CrossRef](#)]
30. Alfaro-Ponce, M.; Cruz, A.A.; Chairez, I. Adaptive identifier for uncertain complex nonlinear systems based on continuous neural networks. *IEEE Trans. Neural Netw. Learn. Syst.* **2013**, *25*, 483–494. [[CrossRef](#)]
31. Chen, L.; Zhu, Y.; Ahn, C.K. Adaptive neural network-based observer design for switched systems with quantized measurements. *IEEE Trans. Neural Netw. Learn. Syst.* **2021**, *34*, 5897–5910. [[CrossRef](#)]
32. Tong, S.; Li, Y.; Liu, Y. Observer-based adaptive neural networks control for large-scale interconnected systems with nonconstant control gains. *IEEE Trans. Neural Netw. Learn. Syst.* **2020**, *32*, 1575–1585. [[CrossRef](#)] [[PubMed](#)]
33. Zhang, Y.; Wang, F. Observer-based fixed-time neural control for a class of nonlinear systems. *IEEE Trans. Neural Netw. Learn. Syst.* **2021**, *33*, 2892–2902. [[CrossRef](#)] [[PubMed](#)]
34. Alzubaidi, L.; Al-Shamma, O.; Fadhel, M.A.; Farhan, L.; Zhang, J.; Duan, Y. Optimizing the performance of breast cancer classification by employing the same domain transfer learning from hybrid deep convolutional neural network model. *Electronics* **2020**, *9*, 445. [[CrossRef](#)]
35. Xie, X.; Fu, C.C.; Lv, L.; Ye, Q.; Yu, Y.; Fang, Q.; Zhang, L.; Hou, L.; Wu, C. Deep convolutional neural network-based classification of cancer cells on cytological pleural effusion images. *Mod. Pathol.* **2022**, *35*, 609–614. [[CrossRef](#)]
36. Kag, A.; Saligrama, V. Time adaptive recurrent neural network. In Proceedings of the IEEE/CVF Conference on Computer Vision and Pattern Recognition, Virtual, 19–25 June 2021; pp. 15149–15158.
37. Perrusquía, A.; Yu, W. Identification and optimal control of nonlinear systems using recurrent neural networks and reinforcement learning: An overview. *Neurocomputing* **2021**, *438*, 145–154. [[CrossRef](#)]
38. Tabanfar, Z.; Ghassemi, F.; Bahramian, A.; Nouri, A.; Shad, E.G.; Jafari, S. Fractional-order systems in biological applications: Estimating causal relations in a system with inner connectivity using fractional moments. In *Fractional-Order Design*; Elsevier: Amsterdam, The Netherlands, 2022; pp. 275–299.
39. Kumar Shukla, P.; Kumar Shukla, P.; Sharma, P.; Rawat, P.; Samar, J.; Moriwal, R.; Kaur, M. Efficient prediction of drug–drug interaction using deep learning models. *IET Syst. Biol.* **2020**, *14*, 211–216. [[CrossRef](#)] [[PubMed](#)]
40. Sahlol, A.T.; Yousri, D.; Ewees, A.A.; Al-Qaness, M.A.; Damasevicius, R.; Elaziz, M.A. COVID-19 image classification using deep features and fractional-order marine predators algorithm. *Sci. Rep.* **2020**, *10*, 15364. [[CrossRef](#)]
41. Matkovskyy, R.; Bouraoui, T. Application of neural networks to short time series composite indexes: Evidence from the nonlinear autoregressive with exogenous inputs (NARX) model. *J. Quant. Econ.* **2019**, *17*, 433–446. [[CrossRef](#)]
42. El-Gohary, A.; Alwasel, I. The chaos and optimal control of cancer model with complete unknown parameters. *Chaos Solitons Fractals* **2009**, *42*, 2865–2874. [[CrossRef](#)]
43. Wang, S.; Bekiros, S.; Yousefpour, A.; He, S.; Castillo, O.; Jahanshahi, H. Synchronization of fractional time-delayed financial system using a novel type-2 fuzzy active control method. *Chaos Solitons Fractals* **2020**, *136*, 109768. [[CrossRef](#)]

44. Zhang, F.; Yang, C.; Zhou, X.; Gui, W. Fractional-order PID controller tuning using continuous state transition algorithm. *Neural Compu. Appl.* **2018**, *29*, 795–804. [[CrossRef](#)]
45. N'Doye, I.; Voos, H.; Darouach, M. Chaos in a fractional-order cancer system. In Proceedings of the 2014 European Control Conference (ECC), Strasbourg, France, 24–27 June 2014; pp. 171–176.
46. Su, Y.; Kuo, C.-C.J. Recurrent neural networks and their memory behavior: A survey. *APSIPA Trans. Signal Inf. Process.* **2022**, *11*, e26. [[CrossRef](#)]
47. Li, Y.; Chen, Y.; Podlubny, I. Stability of fractional-order nonlinear dynamic systems: Lyapunov direct method and generalized Mittag–Leffler stability. *Comput. Math. Appl.* **2010**, *59*, 1810–1821. [[CrossRef](#)]
48. Oldham, K.; Spanier, J. *The Fractional Calculus Theory and Applications of Differentiation and Integration to Arbitrary Order*; Elsevier: Amsterdam, The Netherlands, 1974.

**Disclaimer/Publisher’s Note:** The statements, opinions and data contained in all publications are solely those of the individual author(s) and contributor(s) and not of MDPI and/or the editor(s). MDPI and/or the editor(s) disclaim responsibility for any injury to people or property resulting from any ideas, methods, instructions or products referred to in the content.